Kinetic Modeling of Exciton Migration in Photosynthetic Systems. 3. Application of Genetic Algorithms to Simulations of Excitation Dynamics in Three-Dimensional Photosystem I Core Antenna/Reaction Center Complexes

Gediminas Trinkunas*# and Alfred R. Holzwarth*
*Max-Planck-Institut für Strahlenchemie, D-45470 Mülheim a.d. Ruhr, Germany, and #Institute of Physics, Vilnius 2600, Lithuania

ABSTRACT A procedure is described to generate and optimize the lattice models for spectrally inhomogeneous photosynthetic antenna/reaction center (RC) particles. It is based on the genetic algorithm search for the pigment spectral type distributions on the lattice by making use of steady-state and time-resolved spectroscopic input data. Upon a proper fitness definition, a family of excitation energy transfer models can be tested for their compatibility with the available experimental data. For the case of the photosystem I core antenna (99 chlorophyll + primary electron donor pigment (P700)), three spectrally inhomogeneous three-dimensional lattice models, differing in their excitation transfer conditions, were tested. The relevant fit parameters were the pigment distribution on the lattice, the average lattice spacing of the main pool pigments, the distance of P700 and of long wavelength-absorbing (LWA) pigments to their nearest-neighbor main pool pigments, and the rate constant of charge separation from P700. For cyanobacterial PS I antenna/RC particles containing a substantial amount of LWA pigments, it is shown that the currently available experimental fluorescence data are consistent both with more migration-limited and with more trap-limited excitation energy transfer models. A final decision between these different models requires more detailed experimental data. From all search runs about 30 different relative arrangements of P700 and LWA pigments were found. Several general features of all these different models can be noticed: 1) The reddest LWA pigment never appears next to P700. 2) The LWA pigments in most cases are spread on the surface of the lattice not far away from P700, with a pronounced tendency toward clustering of the LWA pigments. 3) The rate constant k_{P700} of charge separation is substantially higher than 1.2 ps^{-1}, i.e., it exceeds the corresponding rate constant of purple bacterial RCs by at least a factor of four. 4) The excitation transfer within the main antenna pool is very rapid (less than 1 ps equilibration time), and only the equilibration with the LWA pigments is slow (about 10–12 ps). The conclusions from this extended study on three-dimensional lattices are in general agreement with the tendencies and limitations reported previously for a simpler two-dimensional array. Once more detailed experimental data are available, the procedure can be used to determine the relevant rate-limiting processes in the excitation transfer in such spectrally inhomogeneous antenna systems.

INTRODUCTION

In photosynthetic systems, solar energy is absorbed by extended antenna systems, which eventually transfer their excited states in a series of random energy transfer steps to the reaction centers (RCs), where charge separation takes place. The details of the energy transfer processes and the functionally limiting structural factors are not known, except for the simplest of the antenna systems (see Holzwarth, 1987, 1991; Sundström and van Grondelle, 1991; Holzwarth and Roelofs, 1992; Fleming and van Grondelle, 1994; van Grondelle et al., 1994, for recent reviews). There are two main reasons for this lack of knowledge. First of all, the antenna systems are generally too complex, so that even the most sophisticated experiments cannot determine all of the kinetic components and do not reveal the single-step energy transfer processes. Rather, any experiment only measures some derived quantities (lifetimes, time-resolved spectra, etc.), which in themselves contain in a complex and generally nontransparent manner the physical parameters of real interest of the system, i.e., the pairwise energy transfer rate constants and pigment distances and the charge separation rate constant etc. (we previously called them the "hidden parameters"; Beauregard et al., 1991). Second, the detailed structural data for most systems, which are important for their energy transfer properties, are still scarce, although recent experiments promise to provide a good experimental structural basis for a couple of antenna systems (Kühlbrandt and Wang, 1991; Kühlbrandt et al., 1994; McDermott et al., 1995; Karrasch et al., 1995), including PS I (Krauss et al., 1993).

It has long been recognized that one of the most general and important characteristic functional features of photosynthetic antenna pigments is their spectral inhomogeneity (Shiozawa et al., 1974; Freiberg et al., 1987; Jia et al., 1992; Trissl et al., 1993; van der Lee et al., 1993), which needs to be explicitly taken into account if one wants to arrive at a reasonable understanding of the details of the energy transfer processes (van der Laan et al., 1990; Beauregard et al., 1991; Jia et al., 1992; Pullerits et al., 1994; Trinkunas and Holzwarth, 1994a,b).

We have previously presented a detailed two-dimensional lattice model of the energy transfer and charge separation processes in the photosystem I (PS I) core antenna of the

Received for publication 17 August 1995 and in final form 2 April 1996.
Address reprint requests to Dr. Alfred R. Holzwarth, Max-Planck-Institut für Strahlenchemie, Stiftstrasse 34, D-45470 Mülheim a.d. Ruhr, Germany. Tel.: 49-208-3063571; Fax: 49-208-3063951; E-mail: holzwarth@mpi-muelheim.mpg.de.

0006-3495/96/07/351/14 $2.00

W-Pos465

PROTEIN EVOLUTION ON A FOLDABILITY-FITNESS LANDSCAPE.
((**S. Govindarajan** and R. A. Goldstein)) Department of Chemistry and Biophysics Research Division , University of Michigan, Ann Arbor, MI 48109-1055, USA

Evolution determines the shape and function of the biological macromolecules. Understanding the process of molecular evolution can provide insight into the structure and function of these macromolecules and the properties of these molecules will in turn throw light on the process of evolution. We model protein evolution as a random walk in a multidimensional fitness landscape, the configuartion space representing all the possible protein sequences. The fitness of any sequence corresponds to the foldabilty of that sequence to the native state. Foldability being a universal requirement for biological proteins, such a foldability based fitness landscape approach will relate the features of protein structures and evolution. Evolutionary pressure in the form of a minimum foldability requirement was explicitly considered. We observe a phase transition to a slower non self-averaging dynamics in the landscape when the evolutionary pressure is increased. At higher evolutionary pressure sequences tend to evolve along neutral networks stretching across the sequence space, representing particular structures.

W-Pos466

MODELING PROTEIN FOLDING AS DIFFUSION ON ENERGY LANDSCAPES
((**T.-L. Chiu** and R. A. Goldstein)) Department of Chemistry and Biophysics Research Division , University of Michigan, Ann Arbor, MI 48109-1055, USA

The mechanism by which proteins fold into their native three-dimensional structures remains one of the central unsolved problems of molecular biology. Protein folding process is characterized by large *ensembles* of states, whose components depend upon external conditions. In order to approach such a process, recent theoretical work has developed a statistical characterization of the energy landscape of folded proteins. In the present study, we consider folding as diffusion on the energy landscape and use the diffusion equation to study the impact of the nature of the interactions on the folding dynamics. We focus our attention on the relationship between the specific interactions necessary for folding into the native state relative to the average strength of the interactions that result in compaction. The energy landscape is characterized by two different order parameters, one representing the degree of compactness, the other a measure of the progress towards the folded state. We first construct a one-dimensional reaction coordinate through the two-dimensional order-parameter space, compute the free-energy and effective diffusion constant for motion along this reaction coordinate, and then model the folding as diffusion along this coordinate. We find that the optimal average interaction is rather large relative to the distribution of specific interactions, meaning that under optimal conditions proteins would contract quickly and search for their native state from among the compact states.

W-Pos467

FURTHER OBSERVATIONS ON TOTAL HEIGHT/UMBILICAL HEIGHT (H/U): THE GOLDEN MEAN AND FIBONACCI SERIES.
((R.P. Spencer)) University of Connecticut Health Center, Farmington, CT 06030.

As part of a study of osteoporosis in women, we also measured H/U in order to compare the present female population with reported classical Greek measurements. The "Golden mean" dervived from the attempt to divide a line of unit length so that the ratio of the longer segment (L) to the whole line was the same as that of the shorter segment (1 - L) to the longer. Hence L = (1 - L)/L. This solves as the quadratic $(-1 +/- \sqrt{5})/2$, or L = 0.618.. The value of the entire length divided by the longer segment was 1/0.618, or 1.618. The Greek observation was that their H/U was 1.618 or Golden mean. This number is also of interest as it is the ratio in the Fibonacci series (number/preceding number). The Fibonacci series has also been used to describe the growth of certain shelled animals. The value of 1.618 also appears in Chaos theory (Chirikov,B.V.: Chaos, Solitons and Fractals 1:79, 1991). Our study encompassed women without a loss of height, as well as those with a loss of 2 cm or more from osteoporotic collapse (Clin. Nucl. Med. 14:231, 1989). Our population values of H/U ranged from 1.57 to 1.86. "Bending over" or hyperkyphosis of vertebral fractures would decrease H with little change in U, lowering the value of H/U. The present population, likely older and more obese than the ancient Greeks (and probably taller) may have a more mobile umbilicus. More fixed sites, such as the iliac bone height, should likely be utilized.

W-Pos468

A MATHEMATICAL MODEL OF THE CRUSTACEAN STRETCH RECEPTOR.
((**B. Rydqvist** and C. Swerup)). Department of Physiology and Pharmacology, Karolinska institutet, S-171 77 Stockholm, Sweden.

Systems analysis has been applied for the investigation of the input-output relations of the crayfish stretch receptor, a mechanoreceptor analogous to the human muscle spindle. This type of analysis results in mathematical models consisting of a black box with input-output properties similar to the stretch receptor. With increasing knowledge, however, it has become possible to simulate each step in the transduction process between mechanical stimulation and electrical response and in this way create a composite model which gives insight into the transformation at the different stages.
In the present study a mathematical model has been developed of the transduction process in this mechanoreceptor, taking into account the viscoelastic properties of the accessory structures of the receptor (i.e. the receptor muscle), the biophysical properties of the mechanosensitive channels, the passive electrical properties of the neuronal membrane (leak conductance and capacitative properties) and voltage gated ion channels generating impulses. The parameters of the model are derived from studies on the mechanical properties of the receptor muscle, experiments on whole cell recordings of the sensory neuron and from single channel studies of the mechanosensitive channels. The viscoelastic properties of the receptor muscle are modelled by a Voigt element (spring in parallel with a dashpot) in series with a nonlinear spring. The receptor current at different extensions of the receptor was computed using typical viscoelastic parameters for a receptor muscle together with a transformation of tension in the muscle to tension in the neuronal dendrites and finally taking into account the properties of the mechanosensitive channels. The receptor potential was calculated by modelling the neuronal membrane by a lumped leak conductance and capacitance. For the calculation of potential the cell was treated as an idealized spherical body. Voltage gated ion channels were modeled using Hodgkin-Huxley formalism. The model resulted in nonlinear differential equations which were solved by an iterative, fourth order Runge-Kutta method. The performance of the model was greatly improved by introducing an intrinsic adaptation of the mechanosensitive channels. The model can predict a wide range of experimental data from the stretch receptor neurons including the mechanical response of the receptor muscle, the receptor current and its voltage dependence, the receptor potential and the impulse response.

REGULATION OF ION CHANNELS BY HETEROTRIMERIC G PROTEINS

Th-AM-SymI-1 **D. Lambright, University of Massachusetts**
Structural Determinants of G Protein Coupled Signaling

Th-AM-SymI-2 **S. Ikeda, Medical College of Georgia**
Role of G-βγ Subunits in Neuronal Calcium Channel Regulation

Th-AM-SymI-3 **G. Szabo, University of Virginia**
Functional Implications of G Protein Regulated Channel Kinetics

Th-AM-SymI-4 **D. Clapham, Harvard Medical School**
G Protein Gated K^+ Channels

studying adaptation in natural and artificial systems (Holland, 1992). The idea behind the GA is borrowed from Darwinian evolution theory and therefore is quite transparent. In a basic GA (Goldberg, 1989), optimization starts with a random generation of a population of strings, which in a suitable manner encode all parameters describing the system. The strings play the role of chromosomes and the GA operates on the strings of encoded parameters. When decoded, a string describes the parameter sets of the target function to be optimized. In this way every string has to be ranked according to its fitness value in describing the optimum in the target function that must be defined. The ranking mimics the evolutionary selection process and defines whether the particular "individual" will be included in the mating pool or "dies." After the mating pool is chosen, pairs of parents are selected at random from the pool and are crossed over (see below), thus yielding a pair of new individuals of the next generation. This particular operation is of the highest importance. It combines the parent "genes" to produce the offspring chromosome, thus forming an intelligent randomization strategy for the search of the "fittest" population. The offspring, with a small probability, are in addition subject to random mutation (see below). The mutation procedure involves the modification of the genes of an individual 1) to prevent to some extent premature convergence on a suboptimal population and 2) to maintain or increase the diversity of the population. An important aspect is the observation that mutation in the optimization procedure ensures avoidance of being trapped in a local minimum. In the GA the described genetic operations are repeated, either for a predetermined number of times (generations) or until no further improvement in the solution is attained.

The GA's success is based on its implicit parallelism to the search for good solutions by the random sampling of the entire search space with the building blocks of encoded solutions, called *schemata.* The schemata theorem (Holland, 1992) states that from generation to generation the number of fit schemata above average in an infinite population increases exponentially. The GAs have been applied so far to a wide variety of optimization problems and, which is important for our purpose, led to considerable success in providing good solutions for a large class of so-called nondeterministic numerically hard problems (Goldberg, 1989). The classic example of this kind of problem is the traveling salesman problem (TSP) (for a solution by GA see, e.g., Oliver et al., 1987). The hypothetical salesman must visit all of the cities from a given list in an order that minimizes travel. To determine the optimal route, a computing effort that increases exponentially with the number of cities visited is required. A general exact solution does not exist, except for the simplest cases. Fig. 1 shows the basic scheme of the GA applied here to the search for optimal spectral-type distributions of Chl molecules on a lattice. In the following detailed description, every GA element used in this work is discussed.

Definition of fitness

The target function x^{exp} of the specific problem we are simulating here is given by

$$x^{exp} \in x^{exp}[\tau_1^{exp}, \tau_2^{exp}, a_1^{exp}(\lambda), a_2^{exp}(\lambda), I^{exp}(\lambda), \ldots],$$

which consists of experimental time constants (in our special case two), τ_1^{exp} and τ_2^{exp}, their DAS $a_1^{exp}(\lambda_i)$ and $a_2^{exp}(\lambda_i)$, and the steady-state fluorescence spectrum $I^{exp}(\lambda_i)$, at emission wavelengths λ_i (Holzwarth et al., 1993) (the experimental data that are modeled here are exactly the same as discussed in detail by Trinkunas and Holzwarth, 1994a). The aim of the optimization procedure is to describe as accurately as possible this data set by the model simulation. Other experimental data could be added in a straightforward manner if available. The simulation procedure for the theoretical excitation dynamics is based on the Pauli master equation for excitation hopping in a three-dimensional lattice model. The principle of this procedure for the two-dimensional lattice has been described in detail (Beauregard et al., 1991; Trinkunas and Holzwarth, 1994a). All of the parameters required for simulating DAS and steady-state fluorescence spectra, except for the pigment orientation

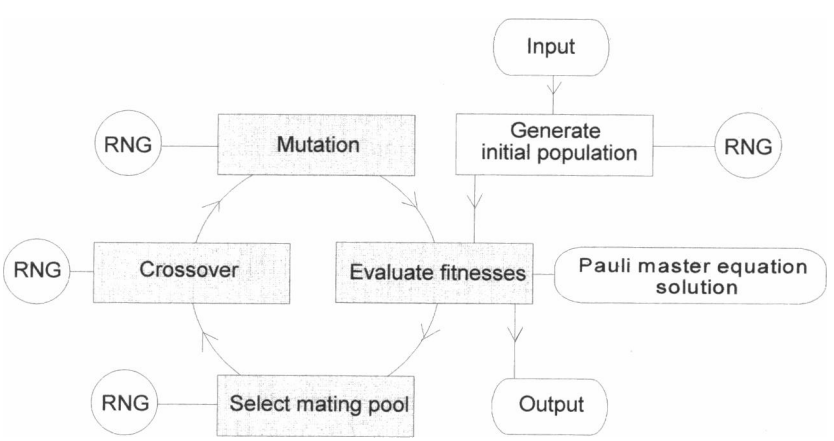

FIGURE 1 Basic scheme of genetic algorithm operations applied to the search for Chl spectral type distributions on a three-dimensional lattice. The input defines the parameterization of the solutions and their encoding. The output yields the final generation of the string population. The abbreviation RNG points to operations that are performed using a random number generator. The RNUNF function of the IMSL (IMSL Inc.) Library was used.

factors, are the same as in the last paper, which treated the two-dimensional lattice (Trinkunas and Holzwarth, 1994a). The objective function for characterizing the fitness F of a particular lattice model described by a particular parameter set is given as follows:

$$F(q^d; q^c) = \left[\frac{1}{N_{exp}} \sum_{i=1}^{N_{exp}} \left(\frac{x_i(q^d, q^c) - x_i^{exp}}{x_i^{exp}} \right)^2 \right]^{-1}, \quad (1)$$

where N_{exp} is the total number of experimental data points. x_i $(q \ldots)$ are the calculated values and x_i^{exp} the experimental values for 1) the two lifetime values (12 and 35 ps) resolved in fluorescence kinetics and 2) the DAS and the steady-state fluorescence spectra (Holzwarth et al., 1993). Equal weighting has been chosen as preferential after testing of the search procedure on simulated data. The function F depends on two kinds of parameters: the discrete spatial distribution parameters q^d of the spectral types on the lattice and the continuous parameters q^c. The permutation p of spectral types on the lattice $p \epsilon L_N$ defines the discrete parameter set q^d. Here L_N stands for the set of all permutations of lattice site labels $l = [1, \ldots, N]$, where N is the number of lattice sites. The lattice constant a, the special distance scaling factors f_{P700} and f_{LWA}, and the intrinsic charge separation rate constant k_{P700} are the continuous numerical parameters q^c.

The problem of finding the optimal spectral lattice and continuous parameter model now can be formulated within the genetic algorithm procedure as:

Maximize: $F(q^d; q^c) = F(p \in L_n; a, f_{P700}, f_{LWA}, k_{P700})$.

An estimate of the total number of different parameter combinations possible for a given encoding scheme is given by the following formula:

$$|L_N| = \frac{N!\, 2^{n_{bit}}}{\prod_{i=1}^{M} s_i!}. \quad (2)$$

Here s_i stands for the number of Chl molecules of spectral type i, M for the number of different spectral types in the model antenna, and n_{bit} for the number of bits used to encode the continuous parameter set. For our lattice model ($N = 100$; $M = 8$; $n_{bit} = 20$) the total number of possible arrangements comes to more than 10^{68}. This shows that our problem of searching for the spectral-type distributions on the lattice is closely related in complexity to the TSP problem, because the search space is formed mainly by the enormous multitude of possible string order permutations. However, the complexity of our task is augmented by the additional necessity to optimize the four continuous parameters of the model, i.e., a, f_{P700}, f_{LWA}, and k_{P700}. Thus, to find the solution it is necessary to search in parallel for optimal parameter sets by the sampling of bit and of order schemata at the same time. We note here that the actual number of free fit parameters in our model is quite low (four continuous parameters plus the parameter describing the spectral ordering, which is formally a single parameter). The latter is a complex parameter, however, and the difficulty of the task is clearly determined almost exclusively by the large number of possible string order permutations.

In addition to the obvious advantage of GAs in optimizing such a complex parameter problem, it is worth noting that we chose the GA for the search for spectral-type distributions for another important reason. The GA, if applied properly, not only results in the single best parameter set but can provide a whole range of (nearly) equally good solutions (if such multiple solutions exist). This feature is optimally in line with our present aim to generate a whole set of different spectral lattice orderings, all reproducing the experimental DAS and steady-state fluorescence spectrum. This is useful for judging how well or how poorly the experimental input data define the parameters of the model and/or how much flexibility the system has in fulfilling the experimental restrictions. Furthermore, this approach is also useful for getting an indication of which additional experimental data would be required to be able to reliably reduce the number of possible (equally good) solutions.

Coding

Following the principle of a minimal alphabet, the continuous parameters in a GA procedure are usually encoded by a bit string. The k bit representation for the continuous parameter q^d with specified lower ($q^d{}_l$) and upper ($q^d{}_u$) bounds allows a precision of $\delta q = |q^d{}_u - q^d{}_l|/(2^k - 1)$. The concatenated bit codes of several parameters then represent a particular individual of the population undergoing evolution. Quite a different coding scheme is required to describe the discrete spectral-type distribution. Because of the necessity of conserving the spectral content of the antenna/RC particle in crossover or mutation, only the spectral-type order can be varied. Thus it is natural to use a coding scheme like the one in TSP (Oliver et al., 1987). In that case, the string representing the spectral-type arrangement on the model lattice consists of lattice site labels $l = [1, \ldots, N]$. The population is then formed by strings that differ in the label order. The translation table $[s] \rightarrow [l]$ for the site labels l and the spectral types s (where $s = [1, \ldots, M]$), defined at the beginning of the search, is then used for decoding of the solutions when their fitness is evaluated.

Selection process

To create the next generation of solutions we made a semideterministic selection of candidates for the mating pool from the preceding generation. This procedure ensures fewer sampling errors than a purely random, roulette wheel selection (Goldberg, 1989). Every string appears in the new population in a number of copies that is determined as the integer part $[K_i]$ of the expected number of individuals K_i,

$$K_i = \frac{KF_i}{\sum_{i=1}^{K} F_i}, \quad (3)$$

where K stands for the population size and F_i for the fitness of the individual I. One additional individual is added to the mating pool with the probability of the remainder of $[K_i]$. In cases of slow convergence, to further reduce the sampling errors, the pair of best individuals of a population was transferred directly to the next generation. After the mating pool is formed, pairs of parent strings are chosen at random for crossover.

Crossover

As described above, we extended the basic GA to perform genetic operations on two string types in parallel. For the crossover of discrete parameter strings (describing the spatial Chl-type distribution), we applied an order crossover operator (Oliver et al., 1987) that transfers only the order information, thus conserving the gene content of chromosomes. Two cut points indicated by vertical dashed lines in Scheme 1 are generated at random. The sections of parent strings between the cut points are copied in a crosswise manner to the offsprings. Then the remaining positions are filled with the genes outside the cut region. Scheme 1 illustrates the crossover operation for a pair of parent strings P1 and P2 containing 10 genes (A to J). The transfer of the cut section to the partner string produces holes in the parent string, which are collected in the cut section while sliding the remaining genes from the right to the left. Finally, the offspring strings O_1 and O_2 are obtained by swapping the contents of the corresponding cut sections. For this kind of crossover it is characteristic that both the absolute and the relative positions of the parent genes are combined to produce the offspring.

For the crossover of bit strings encoding the continuous parameter set, we also start with a random choice of two crossing points, and the offspring are formed simply by swapping the cut sections.

Mutation

In our search procedure the mutation procedure was implemented as follows. First, with some predefined probability a pair of lattice sites was chosen at random. If the spectral types of these sites were found to be different they were exchanged; otherwise the random choice was repeated until it was successful. The same procedure was also applied to the continuous bit string. Notwithstanding the minor role the mutation was expected to play in the search procedure, during the test runs carried out to find the optimal mutation probability, a slight but significant influence of this parameter on the diversity of population produced has been observed.

Search for subpopulations

Unfortunately, the above-defined modifications of the basic GA are still not sufficient to achieve our aims. If applied they would result in convergence of the search to a single "best lattice arrangement" with respect to positions of P700 and the LWA pigments. Thus the whole population evolves to a set of very similar strings. This would be inconsistent with our aim of including a whole set of different "good" solutions in our final population. To increase the diversity of the string population we also applied the so-called sharing procedure (Goldberg and Richardson, 1987). This procedure induces a higher string diversity in a population by deliberately reducing the fitness for strings that are very similar. To achieve this aim, strings I and j are compared position by position, and the number of different genes d_{ij} is counted:

$$d_{ij} = \sum_{k=1}^{N} (1 - \delta_{s_{ik}, s_{jk}}), \tag{4}$$

where δ stands for the Kronecker delta function. Every string of a population is then characterized by the vector of nonlinear sharing functions (Goldberg and Richardson, 1987):

$$Sh_{ij} = \begin{cases} 1 - (d_{ij}/\sigma)^{\alpha}, & d_{ij} \le \sigma \\ 0, & d_{ij} > \sigma \end{cases} \tag{5}$$

where α represents the nonlinearity parameter of the sharing extent and σ defines the cutoff limit for the amount of difference between two strings. In our problem σ has a simple interpretation. It essentially defines which sites of the lattice are the most important ones for the optimization and should be included in the forced formation of stable subpopulations, thus inducing natural niche-like behavior. By using this sharing function, the fitness of a string of the population is reduced in dependence on its homology:

$$F_i' = F_i \left(\sum_{j=1}^{K} Sh_{ij} \right)^{-1}. \tag{6}$$

Without this procedure the population converges essentially on one particular spectral arrangement. It should be noted that the sharing procedure is highly problem dependent, and

P1 ≡ ABCD	EFG	HIJ		●B●D	EFG	●IJ		DEFG	●●●	IJB	O1 ≡ DEFG	CAH	IJB
			⇒				⇒				⇒		
P2 ≡ IEJD	CAH	GBF		I●JD	CAH	●B●		DCAH	●●●	BIJ	O2 ≡ DCAH	EFG	BIJ

Scheme I

thus both sharing function parameters must be tuned for every particular optimization problem.

Testing of the procedure

The described search procedure was tested on synthetic DAS simulated for a small square model lattice. Because of the symmetry of a square lattice, the spectral lattice arrangements are potentially fourfold degenerate. It was found that the sharing procedure adopted in the search for the string orderings worked quite well in revealing all four degenerate arrangements. However, some tuning of the search parameters, i.e., crossover and mutation probabilities, selection type, etc., for our particular problem was required. It was found already for the small test lattice that the population diversity was higher for larger populations. To reduce the search space to the necessary minimum in the actual optimization runs, the symmetry degeneracy of the lattice was removed by keeping the P700 pigment site in a $2 \times 3 \times 3$ sublattice located in one corner of the $4 \times 5 \times 5$ lattice. If because of crossover or mutation P700 were to leave this predetermined area, it is immediately returned at random to a position within the allowed area. This operation increases to some extent the effective mutation rate. However, we found that it has a minor disturbing effect only on the optimization, because the mutation as well as crossover rates, sharing function parameters, population size, and number of generations, are the decisive parameters determining the optimization convergence and population diversity, which had to be determined empirically for the particular problem anyway. It is obvious that in a complex optimization problem such as the one given here the size of the parameter space should be kept at the necessary minimum by taking into account all existing symmetry relationships.

We started with the matrix of excitation transfer rates as calculated for the regular lattice with lattice constant $a = 1.5$ nm, because this corresponds to the upper lattice spacing limit already predicted by the PS I x-ray structure experiment (Krauss et al., 1993) as well as by two-dimensional lattice modeling (see Trinkunas and Holzwarth, 1994a).

The preliminary search runs were necessary to set up the limits for the continuous parameters. For the factors f_{P700}, f_{LWA}, and f, which scale the pairwise transfer rates (via scaling of the distances) involving P700, LWA, and the main pool pigments, respectively (the scaling factors are ordered above in the sequence that defines the priority of actual pairwise excitation transfer rate scaling), they showed that during the population convergence the parameters f_{P700} and f_{LWA} were never lower than 1, and f was always higher than 0.1 for the optimal solutions. Furthermore, these parameters always stayed well below the upper bounds of 60, 60, and 6, respectively, which were chosen as limits in the final runs. For the charge separation rate k_{P700}, the range of $1.0-6.0\ ps^{-1}$ has been determined to be the optimal range. The lower bound is lower than the theoretical limit of the infinitely fast migration case (trap-limited decay) when the lowest momentum of the excitation decay function (LMD) is exclusively determined by the trapping part (see Eq. 8 below). The choice of the upper bound approximately represents the other extreme of the excitation decay rate-determining limit when the migration contribution dominates the LMD (migration-limited decay). The final simulation runs showed that the choice of these parameter ranges, which were based on the one hand on the preruns with lower resolution and a wider range of allowed parameter changes, and on the other hand on the the theoretical considerations described above, was never really limiting. Thus only in the case of the NN approximation (see below) did one parameter, i.e., the rate k_{P700}, approach the upper limit, but no other parameter did in any of the three models. In general, the narrowing of the allowed intervals for the parameters, based on the preruns, is very important because it enables us to use a smaller number of bits per parameter without a loss of accuracy. This facilitates considerably the overall convergence of the search procedure. Using five bits each per parameter as coding then corresponds to a resolution of 59/32, 59/32, 5.9/32, and 5./32, respectively, for these parameters. All of the 20-bit strings for these continuous parameters for the initial population were then generated at random. The suitability of the above choices was confirmed by the final simulations (see below).

Because the search for the P700 spectral-type position was performed in a limited part of the lattice only (see above), the sharing parameter was chosen to be $\sigma = 3N/4$. The motivation for this choice comes from the number of different lattice sites that can be occupied by P700 and can be accessed in a pairwise excitation transfer step. We found the sharing procedure to operate best at a nonlinearity parameter $\alpha = 0.1$ (Eq. 5).

In the course of test runs we found that for a proper search for good permutations of 100 pigments, we needed to include about 1000 strings in a population. Further increase of the population size did not improve the search considerably. The main improvement in finding new spectral lattice arrangements as well as in fitness was usually achieved in about 100 generations, whereas further search was considerably slower (Holzwarth and Trinkunas, 1994b). The probabilities of 0.65 for the spectral type string crossing and 0.003 for the gene mutation were found to be optimal with respect to the overall procedure convergence and the desired induction of population diversity. The same probabilities were used for the crossing and mutation of bit strings of continuous parameters.

RESULTS

Model 1: nearest-neighbor transfer approximation (NN)

First we performed searches for three-dimensional lattice spectral arrangements within the widely used nearest-neighbor (NN) transfer approximation, which we also used previously in

the simulation of the two-dimensional lattice model (Trinkunas and Holzwarth, 1994a). The extension of the permutation search to the parallel search of bit strings coding for the continuous parameters unfortunately increases the stochastic jumps in the sampling of the total parameter space, as can be seen, e.g., in Fig. 2. This is partly due to the fact that the size of the population (1000) was still relatively small. Therefore, as can be seen in Fig. 2, the trace of the individual with best fitness (*solid line*) is "noisy." A reasonable fit level indicated by the dashed line parallel to the x axis is reached in about 40 generations. The average fitness (also *solid line*) never reaches the reasonable fit level, thus indicating that in the final generation only a small part of the population (~10%) is adapted to the fitting requirements. This result is a consequence of the intentional property that the entire population is under the constant pressure of the sharing procedure (see Methods) to search for a large number of different solutions, in agreement with our fitting aims.

The result of this pressure for a large genetic variety are nine spectral lattice arrangements differing in the mutual arrangements of P700 and LWA pigments. It is characteristic that the LWA pigments are always found to be spread on the surface of the lattice. In these nine different arrangements the type 6 pigment appears next to P700 five times, whereas the type 7 pigment never does. The P700 in three cases is also found on the surface. All occurrences of P700 and LWA pigment clusters appearing in the final generation are listed in Table 1. In spite of the fluctuations the tendencies of the continuous parameters (for the best individual in each generation) in the course of the evolution can be clearly seen (cf. Fig. 3 *A*). The main lattice constant a is slightly reduced compared to the initial value of 15 Å. The distances between the P700/LWA pigments and their nearest neighbors fluctuate slightly about their mean values

TABLE 1 Clustering of the RC and the red pigments observed in the final generations

Cluster type/lattice	NN	NNN	NNNR
6–6	●		
6–7	●	●	
RC-6; 6–7	●		●
RC-6–6		●	
6–6-7	●	●	
RC-6; 6–6-7	●		
6–7; RC-6–6		●	●
6–6; 6–6-7		●	
6–6-6–7*			●
RC-6; 6–6-6–7			●
6–6-6–6-7*			●

*Penetration of type 6 pigment into the lattice.
NN, nearest-neighbor transfer approximation; NNN, next to nearest neighbor transfer approximation; NNNR, the same as NNN, with the RC site fixed in the center of lattice side surface. A dash between the numbers means that the corresponding spectral types are direct neighbors.

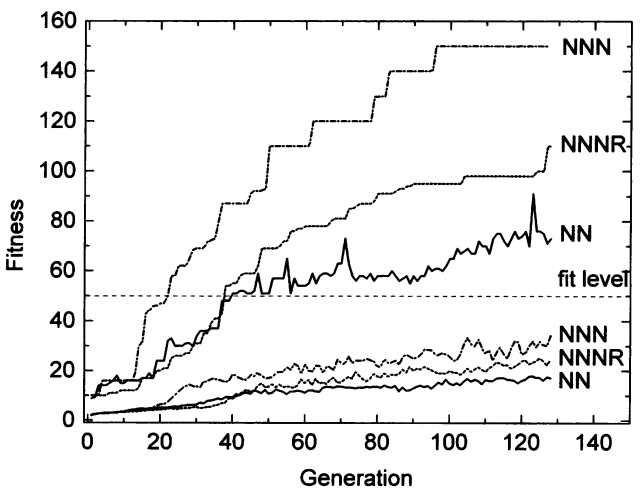

FIGURE 2 (*Upper curves*) Evolution of the fitness for the best individual of the population for the three cases: NN, nearest-neighbor pairwise excitation transfer only; NNN, pairwise excitation transfer now including also the next to nearest-neighbor sphere; NNNR, the same as NNN, with the P700 site fixed in the center of the 5 × 5 surface plane of the three-dimensional lattice of dimensions 4 × 5 × 5. (*Lower curves*) The evolution of the average fitness of the population in the corresponding approximations indicated above. The horizontal dashed line indicates the good fitness level, above which the distributions are considered as describing sufficiently well the experimental fluorescence kinetic data (Holzwarth et al., 1993).

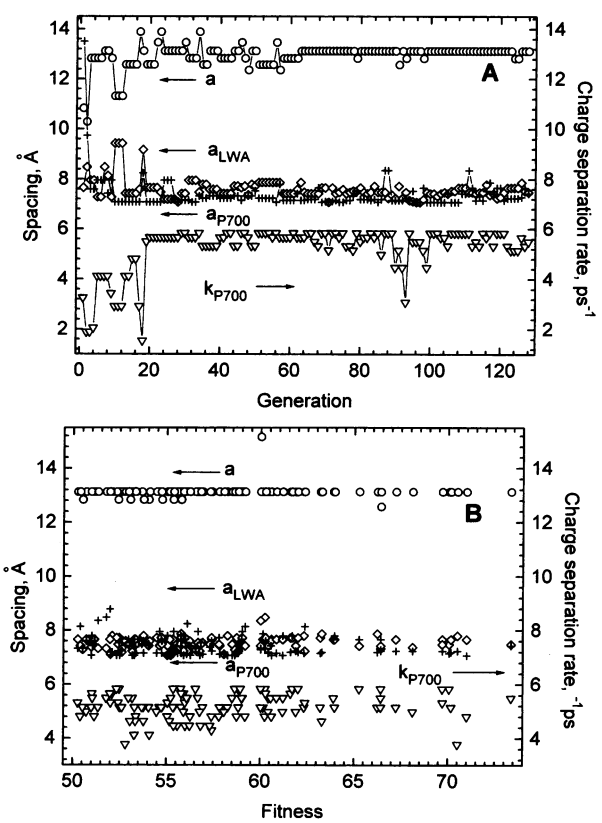

FIGURE 3 Case of nearest-neighbor pairwise transfer approximation (NN). (*A*) Evolution of the continuous parameters (lattice constant a, spacing between the P700 and the main pool pigments $a_{P700} = a l f_{P700}^{1/6}$, spacing between the LWA pigments and the main pool pigments $a_{LWA} = a l f_{LWA}^{1/6}$, intrinsic charge separation rate k_{P700} for the best individual of the population. (*B*) Distribution of the above-mentioned parameters for the good members of the population in the final generation of the search.

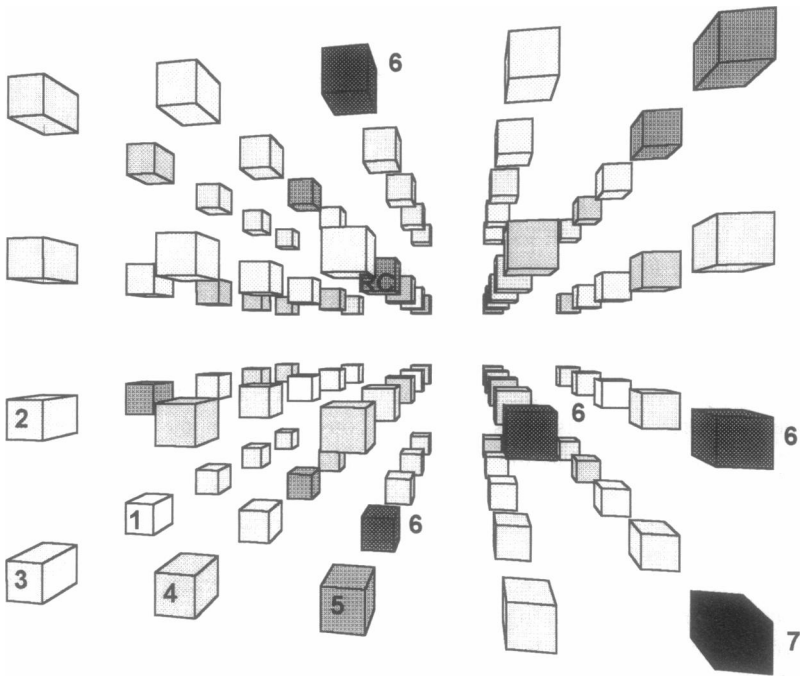

FIGURE 4 The optimal spatial distribution of the pigment spectral forms in the three-dimensional lattice of the PS I core particle, as obtained by the genetic algorithms in the NN approximation. The optimal values for the continuous parameters are as follows: Charge separation rate $k_{P700} = 3.8\ ps^{-1}$, lattice constant $a = 13.1$ Å, spacing between the P700 and the main pool pigments $a_{P700} = 7.2$ Å, spacing between the LWA pigments and the main pool pigments $a_{LWA} = 7.8$ Å. For the spectral content of the model see the section on model parameters. The seven different grey levels (the P700 site is indicated by the label RC) positively correlating with the absorption maxima of Chl molecules are used to distinguish among the different spectral types.

a_{P700} and a_{LWA}, which are both reduced considerably compared to the main lattice constant a. The charge separation rate of the best individual k_{P700} also fluctuates close to the limiting value determined by the upper bound. In Fig. 3 *B* the distribution of the continuous parameters for the good solutions of final generation is presented. It is clearly seen that for the optimal lattice arrangements (those of large fitness) the increase in pigment density, i.e., the decrease in lattice distance, around P700 and the LWA pigments is a characteristic feature. In spite of a clear tendency toward very fast charge separation rates of 5–6 ps^{-1}, a few individuals with significantly smaller values are also present. Fig. 4 shows the optimal spectral lattice arrangement with the slowest charge separation rate. In this case the migration time amounts to ~70% of the excitation lifetime. (In this work it was determined from the intercept of the linear dependence of the LMD on the inverse charge separation rate; see Eqs. 7 and 8 below.) In that case the migration time simply equals the first passage time (FPT) (for a definition see, e.g., Weiss, 1967).) This indicates that essentially a migration-limited charge separation process is characteristic for the NN approximation model. We note, however, that this model is too simple and has only been included here for the sake of comparison with previous simulations that were based on this approximation.

Model 2: next to nearest neighbor transfer approximation (NNN)

In this model the second coordination sphere of neighboring pigments is also included in the calculation of the energy transfer rates and the solution of the master equation. The relaxation of the simple NN approximation somehow unex-

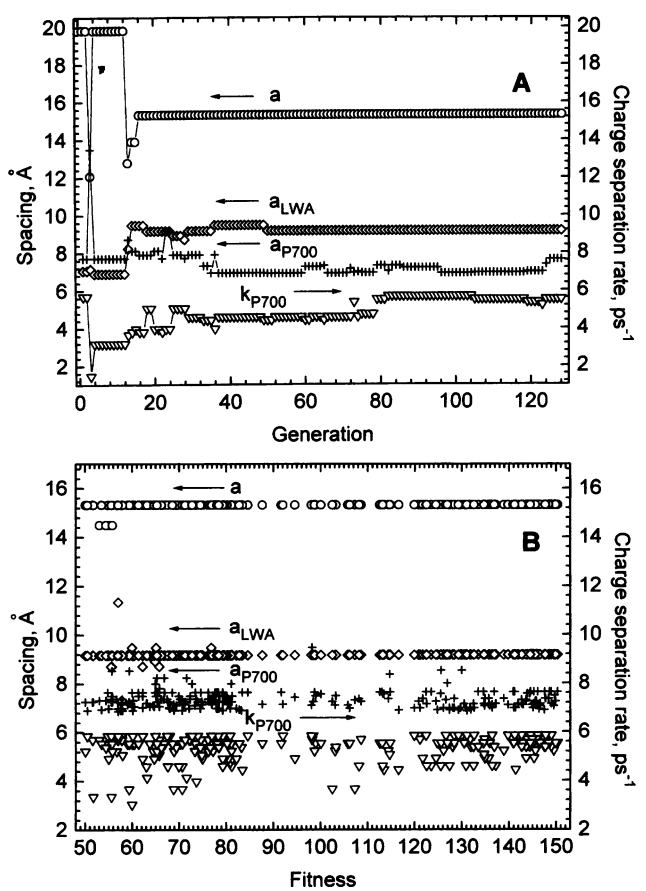

FIGURE 5 Next to nearest neighbor pairwise transfer approximation (NNN). (*A*) Evolution of the continuous parameters. (*B*) Distribution of these parameters for the good solutions in the final generation of the search. All of the definitions are the same as for Fig. 3.

pectedly slowed down considerably the convergence toward a good fit level and showed less diversity of solutions in the population. Therefore, to speed up the evolution we applied an "elitist selection" modification that involved the automatic transfer of the best pair of individuals to the next generation without changes. This immediately improved the performance of the GA procedure, and the level of good fits was crossed in about half the number of generations that was needed in the former case (Fig. 2). The traces of the evolution of the continuous parameters (Fig. 5 *A*) are considerably less noisy and involve several changes as compared to the traces of Fig. 3 *A*. The considerable increase in the lattice constant as compared to the NN case (Fig. 3) and the slight increase in the distances between the LWA pigments and the nearest neighbors are evident. However, the feature of a high charge separation rate for the best individual remained basically unchanged. Furthermore, the distribution of the continuous parameters for the good solutions in the final generation (Fig. 5 *B*) indicates the regular spread of these parameters around the values of the best individual in the last generation. In contrast to the run based on the NN approximation, the total number of individuals with good fitness is now twice as large. In the final generation, again nine different mutual arrangements of P700 and LWA pigments were found. The P700 in four of these cases was found on the edge of the lattice. The type 7 pigment again was never found next to P700, whereas the type 6 pigment was always present on the first or the second coordination sphere of P700. The clustering of LWA pigments is more pronounced as compared to the NN case (see Table 1). The lattice arrangement possessing the slowest charge separation rate is shown in Fig. 6. Again the estimate of the contribution of the migration time to the LMD for this lattice gives a high value (72%), indicating that for all of the optimal solutions of the next to nearest neighbor (NNN) model, a more migration-limited charge separation process applies.

Model 3: P700 site fixed in the center of one of the lattice surface planes (NNNR)

The models described above considered the P700 site position to be a free fitting parameter, just as all remaining pigment positions were. Based on the recent structural data on PS I (Krauss et al., 1993), P700 seems to be located in the center of protein close to the surface at the lumenal side of the membrane. Fixing the P700 site in the center of the lattice surface plane (dimensions 5×5) is expected to be advantageous for the search for models with the shortest migration times.

In spite of the elitist selection, the convergence of the best individual fitness for this case was not as fast (Fig. 2) as in the NNN case. However, this time the charge separation rate converged to a value close to the center of the interval of possible values rather than to the upper bound value (Fig. 7 *A*). The lattice constant a converged to almost the same value as in the NNN case. The distance between the LWA and main pool pigments evolved toward the lattice constant a of the main pool pigments, whereas the distance from P700 to its nearest neighbors was found to be again half the value of a, similar to what was found for the NNN case (see Fig. 5).

The individuals with good fit in the last generation covered the high proportion of 22% of the whole population. Twelve different pigment spectral form distributions with respect to P700 and LWA pigments were found in this case. They followed patterns similar to those described above, but larger clusters were more frequent (Table 1). The continuous parameters for the good fit individuals were again distributed narrowly around the corresponding values of the best individual (see Fig. 7 *B*). For the distances between P700 and its nearest main pool pigments, this distribution covers values from 7 to 9 Å. Notably, for the first time in any of our simulations, several charge separation rates were found to be lower than 2 ps^{-1}. It is interesting that four of six such lattices are different with respect to their P700-to-LWA pigment arrangement, showing in particular two different type 7 pigment locations. One of these lattices is shown in Fig. 8. In that case, the migration time contributes only 42% to the LMD and can thus be regarded as a more trap-limited excitation transfer model.

DISCUSSION

By testing three different lattice models using the GA procedure, we obtained over 400 spatial distributions of spectral types on the three-dimensional lattice that describe well the experimental kinetic fluorescence data (Holzwarth et al., 1993). A large fraction of them differ only in the arrangement of the main pool pigments, and many of them could be rejected as reasonable solutions if precise decay data on the subpicosecond time scale were available. Thirty of these good fit arrangements differ only in the mutual arrangement of P700 and LWA pigments, which are the most decisive parameters in the model. Thus at present, without more experimental information on kinetics at the subpicosecond time scale, it is not possible to further reduce the range of possible solutions. However, it is important that all of the LWA pigment arrangements found up to now possess several common characteristic features, providing a new insight into the spatial organization of the spectral forms in the core antenna of PS I. The general finding that about 10 different good arrangements are obtained per population of 1000 is also understandable. As a rough estimate, to form the stable subpopulations in a GA run, it is necessary to have a sampling statistics (number of individuals) of at least 100 per different mutual arrangement of P700 and LWA pigments. However, in most of our simulations just two or three individuals out of the total population with at least good fitness possess a population on the order of about 100, whereas the others are represented to a considerably smaller extent. This means that the latter arrangements are only

marginally represented in the population. One reason could be some nonoptimally tuned procedure parameters, although we believe this to be unlikely in view of the fact that we have extensively tested the procedure. A more likely reason in our view is the fact that to achieve more stable subpopulations, a considerable increase in population size would be required. Unfortunately, this can be achieved only at the expense of extremely high computation time. For our typical cases one evolution run on an Alfa-station DEC-3000-400 took at least 24 h. The following finding may give a hint toward this limitation. The spectral-type distribution of the lattices with the P700 site fixed in the center of the surface plane should be fourfold symmetry degenerate (in that case we did not limit the search to one of the symmetry-related solutions only). However, symmetry-related equivalent distributions did not appear in the final generation. This indicates to some extent that our search procedure at the given population size is not fully capable of developing all possible spectral-type distributions. The origin of that problem is based on the extremely large space of the spectral-type permutation string and the comparably small population sizes that can be used without going to excessive computation times. Nevertheless, the search procedure based on the genetic algorithm performed quite well in also discovering the more trap-limited models when the search space has been limited by imposing a restriction on the P700 site location (NNNR approximation) or when the procedure was explicitly pressed to search for solutions with a minimal k_{P700}.

The main disadvantage of the GA search procedure is that in principle every new problem requires that the search parameters be tuned specifically to that problem. Furthermore, for a proper search in a problem with very large parameter space, very large population sizes are required concomitantly, which in turn means high memory and processor time resources. Clearly, parallel computing would be an ideal solution for the latter problem.

Features of the optimal spectral lattice arrangements

It is important to note that all 30 of the different above-discussed lattice patterns concerning P700 and LWA pigments as well as many others that we found during this study follow several characteristic features. First, the reddest LWA pigment never appears next to P700 (see Table 1). This result is in contrast to a common view about the optimal location of LWA pigments in PS I cores in particular and in spectrally inhomogeneous antenna/RC systems in general (see van Grondelle et al., 1994, and references therein). Second, the LWA pigments in most cases are spread on the surface of the lattice not far away from P700 (see, e.g., Figs. 4, 6, and 8).

To better understand how these arrangements emerged we ought to discuss the limiting factors for the pigment arrangement. We refer therefore to the expression for the LMD in the homogeneous lattice (Pearlstein, 1982; Valkunas et al., 1986), which can be generalized to the spectrally inhomogeneous lattice model (Trinkunas and Holzwarth, manuscript in preparation):

$$\tau_0 = \tau_{FPT} + \tau_{trap}. \tag{7}$$

The average first passage time τ_{FPT} (Weiss, 1967) stands for the migration part of the LMD. (For the treatment of the migration term in the case of a heterogeneous antenna, see Somsen et al. (1994) and Somsen (1995).) The term τ_{trap} denotes the trapping part, i.e., the excitation survival (or residence) time in the antenna in the case of infinitely fast excitation migration. It can be expressed by the following exact relationship:

$$\tau_{trap} = \frac{1}{k_{P700}} \sum_{i=1}^{N} \exp\left(- \frac{\epsilon_i - \epsilon_{P700}}{k_B T} \right), \tag{8}$$

where N stands for the number of pigments in PS I; ϵ_i denotes the excited state energy gap for the pigment i; k_B stands for the Bolzmann constant; and T denotes the absolute temperature. The part comprising the sum denotes the inverse of the P700 pigment population in the hypothetical case of thermal equilibrium. Note that in contrast to Eq. 8, the trap-dependent part of the longest lifetime in the general case of a spectrally inhomogeneous antenna/RC particle has no closed analytical expression (Laible et al., 1994), however, and that τ_{trap} in Eq. 8 is not the longest lifetime in the system. It is worth to noting, however, that for the spectral-type distributions compatible with the kinetic experimental data at room temperature, we did not find very significant differences between the values of the LMD and the longest-lived component.

The amplitude of the equilibration component of the experimental DAS around 690 nm is about 1.5 times larger than the amplitude of the main trapping component at this wavelength (Holzwarth et al., 1993). This means that initially (and after some rapid equilibration in the main pool; Du et al., 1993) the main pool pigments are losing their excitation, mainly because of transfer to the LWA pigments. To a lesser extent their excitation is directly trapped by P700. To reduce the direct trapping by P700 during the GA evolution run, the LWA pigments are moved away from P700 to the surface, where the site coordination number is smaller and the excitation has a higher chance of residing for longer times. However, this is in conflict with the consequence that τ_{FPT} now becomes longer. In turn, this creates pressure to increase the charge separation rate or to reduce the lattice constant to shorten the migration times. This network of coupled relationships forms the landscape on which the search for good solutions in the GA procedure occurs.

It is understandable that the relaxation of the nearest-neighbor (NN) approximation resulted in an increase in all of the lattice distances. Because of the stronger mutual dependence of the parameters in the NNN and NNNR

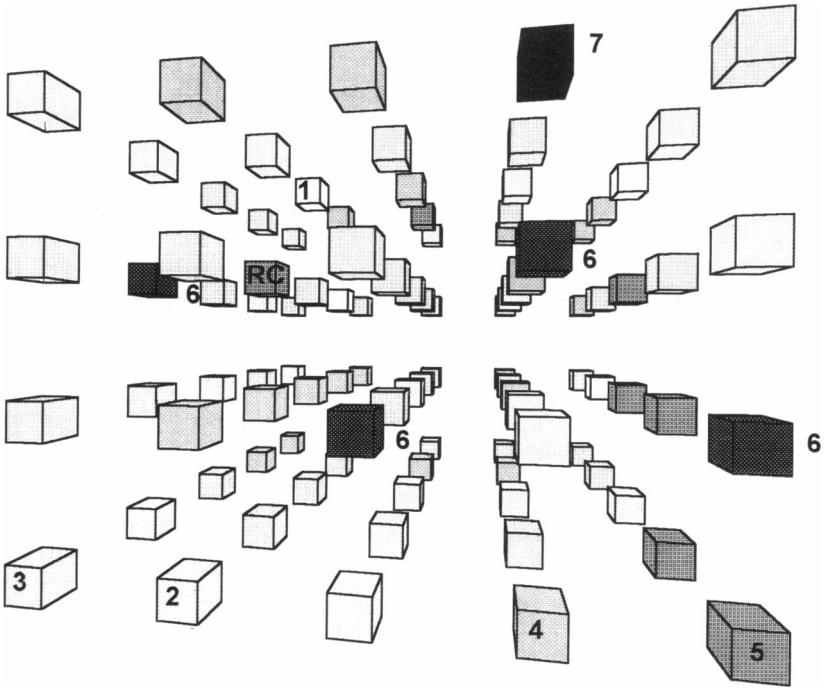

FIGURE 6 The optimal spatial distribution of the pigment spectral forms in the three-dimensional lattice model of PS I core particle, as obtained by genetic algorithm in the NNN approximation. The optimal values for the continuous parameters are as follows: charge separation rate $k_{P700} = 3.7\ ps^{-1}$, lattice constant $a = 15.3$ Å, spacing between the P700 and the main pool pigments $a_{P700} = 7.3$ Å, spacing between the LWA pigments and the main pool pigments $a_{LWA} = 9.2$ Å. For the spectral content see the explanations in Fig. 4.

approximations, the convergence for the fitness of the best individual considerably slowed down, however (not shown). Nevertheless, the use of the elitist selection procedure speeded up the convergence significantly (Fig. 2). However, from Table 1 it can be seen that a higher extent of the clustering for the LWA pigments is now a characteristic feature. When, to shorten the FPT, the P700 site was fixed in the center of the square surface plane (NNNR model), probably because of severe limitations for the above-discussed parameter relationships, the convergence of the fitness for the best individual was again slowed down. This effect of imposing restrictions resulted again in a further increase in clustering of LWA pigments (Table 1). However, most importantly, this time we succeeded in obtaining a model (see Fig. 8) in which the excitation is spending less than half of the total decay time in the antenna. Quite interestingly, in the final population six individuals appeared with rates of k_{P700} closer to the lower theoretical limit ($1.2\ ps^{-1}$) of the intrinsic charge separation rate (see Fig. 7 *B*). Thus a tendency to a more trp-limited kinetics appears in the NNNR model, in contrast to the NN and NNN models. From a structural point of view (Krauss et al., 1993), as already mentioned above, the NNNR model with its P700 placing at the surface of the particle would seem to be the most adequate for PS I of all the models tested here.

The high clustering of LWA pigments probably reflects the expected tendency that a compact arrangement of P700 and the LWA pigments is favorable for a shorter migration time and thus allows a relatively longer charge separation time. This could possibly also serve as some indication of a dimeric LWA pigment origin, as was suggested from a fluorescence study of PS I from the cyanobacterium *Synechocystis* at liquid helium temperatures (Gobets et al., 1994). It is important to note that the last two search runs indicate that distances from the LWA pigments to the other pigments are slightly shorter as compared to the main lattice constant, thus indicating some structural inhomogeneities of pigment density at the LWA pigment sites. This result could alternatively be interpreted as a more favorable mutual orientation of transition moments, because we used a fixed average orientation factor in our simulations. However, because the rate constants scale with the sixth power of the inverse distance, it is unlikely that a more optimal orientation factor could be the only cause of the higher transfer rates. Nevertheless, the LWA pigments always appear in a few separate locations.

Van Grondelle et al., in their recent review article (van Grondelle et al., 1994), based on an interpretation of PS I-100 x-ray structure (Krauss et al., 1993), suggested that around the RC pigment(s) there occurs some increased spacing to the nearest surrounding antenna Chls, i.e., very similar to that in photosynthetic bacteria (Somsen et al., 1994). It is thus important that in our simulations we never obtained any indication whatsoever of a reduced pigment density around P700, although the search was completely free to increase the distance of the nearest surrounding Chls to P700. In fact, not a single arrangement found during the preliminary and final optimization runs showed such an increased antenna-P700 separation. Furthermore, we specifically searched by fixing the distance from the nearest-neighbor pigments to P700 at 1.5 times the average lattice constant. In this simulation, which ran over 128 generations, the best individuals fitness reached just less than 20% of the good fitness level threshold.

We would like to note here that the optimized model parameters for the core also shed some light on the problem

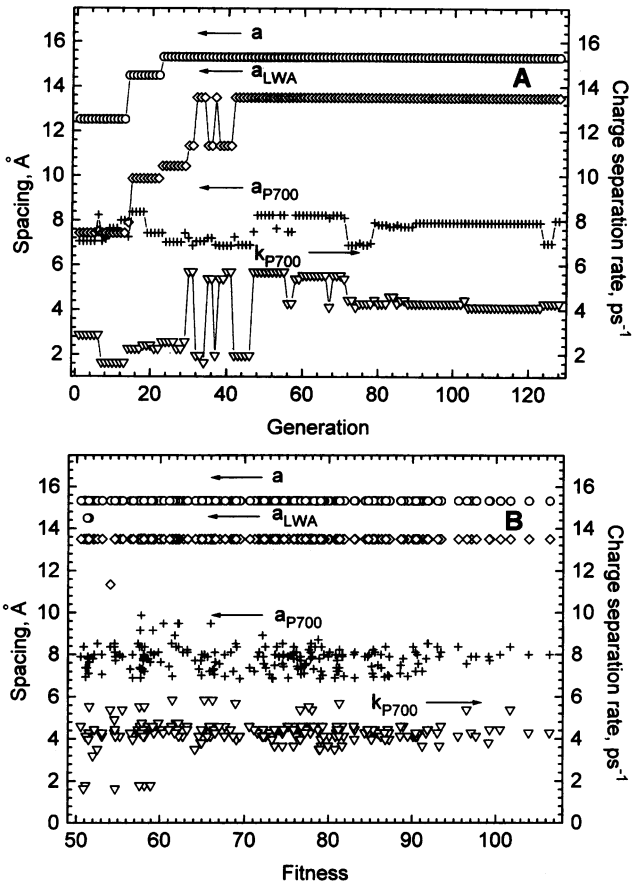

FIGURE 7 Next to nearest neighbor pairwise transfer approximation with P700 site fixed in the center of the lattice surface plane (NNNR). (*A*) Evolution of the continuous parameters. (*B*) Distribution of these parameters for the good solutions in the final generation of the search. All of the definitions are as in Fig. 3.

of excitation trapping in the native PSI-200 complex, where it is believed that the LWA-most absorbing pigment is situated in the periphery on the light-harvesting complex I. The general insights and arrangements obtained in this work could also serve as approximate models for the PS I-200 organization. Our simulations prove that the location of the LWA pigment(s) relatively far from P700 does not create any problems with respect to efficient trapping.

The intrinsic rate of charge separation from P700

There is some tendency in the literature to expect that the intrinsic charge separation rate k_{P700} in PS I to be similar to that from the bacterial RC, i.e., about 0.3 ps^{-1} (Parson, 1991). Our simulations clearly do not support this view, because the lowest charge separation rate that could be obtained in our simulations, even when putting a high pressure on the optimization routine to search for slow charge separation, was above 1 ps^{-1}. One might argue that the model is somehow not properly adapted to allow this result. This can be excluded, however, because there is a very simple and straightforward way to test this quite independently of any complex model. As can be seen from Eq. 8, the lower bound for the charge separation rate can be estimated on the basis of the hypothetical thermally equilibrated excitation decay in an antenna/RC particle (Trissl, 1993; Lin et al., 1994; van Grondelle et al., 1994). Thus the lower bound of the intrinsic charge separation rate, for a given system and the corresponding set of lifetimes, is defined by the spectral content of the system and by the temperature. Under the conditions given here, this results in a lower rate limit of 1.2 ps^{-1}. It is thus understandable why previous simple compartment models of PS I never revealed the problem with the fast charge separation rate. The relatively free choice of the charge separation rate in these simple models was only possible because of the fact that these compartment models generally did not apply a realistic spectral content, i.e., a realistic inhomogeneous distribution function for the antenna Chls. Therefore the lattice model (Fig. 8) with a charge separation rate of 1.8 ps^{-1} (NNNR approximation) is very close to the theoretical limit and implies a more trap-limited kinetics.

CONCLUSIONS

It has been shown that the GA procedure is indeed a suitable and powerful method of optimizing the parameters for the structure and the energy transfer rates in a complex antenna system in accord with experimental input data. The GA procedure represents an important step forward, as compared to a pure manual random search for optimal arrangements as done previously. As expected, a variety of equally good parameter sets resulted from the GA runs. A manual search in a three-dimensional lattice would clearly have failed entirely in revealing this substantial variety in good parameter sets. These parameter sets have some common and quite characteristic features, however, with respect to the relative arrangement of P700 and LWA pigments and the clustering of LWA pigments. The longest wavelength-absorbing pigment was never found in the direct vicinity of P700, and we can exclude a reduced antenna pigment density around the P700 pigment.

The present results show that the present experimental data are consistent in principle with both more migration-limited and more trap-limited transfer models (see, e.g., Figs. 6 and 8, respectively), depending on which limitations are put on the models. However, the extreme migration-limited and the extreme trap-limited models can be clearly excluded. A final decision between the various models is not possible at present, based on the limited amount of available experimental input data. Detailed high time resolution transient absorption and/or fluorescence data (time resolution below 1 ps) are required to decide which of these situations is actually realized in the PS I core antenna. However, if one accepts that the NNNR model is the most suitable description of PS I, then the tendency toward a more trap-limited kinetics is clearly indicated by the simulations. Once further experimental data are available, the currently large number of possible solutions can be narrowed down substantially. Nevertheless, it appears possible that not just a single solution will eventually emerge, but

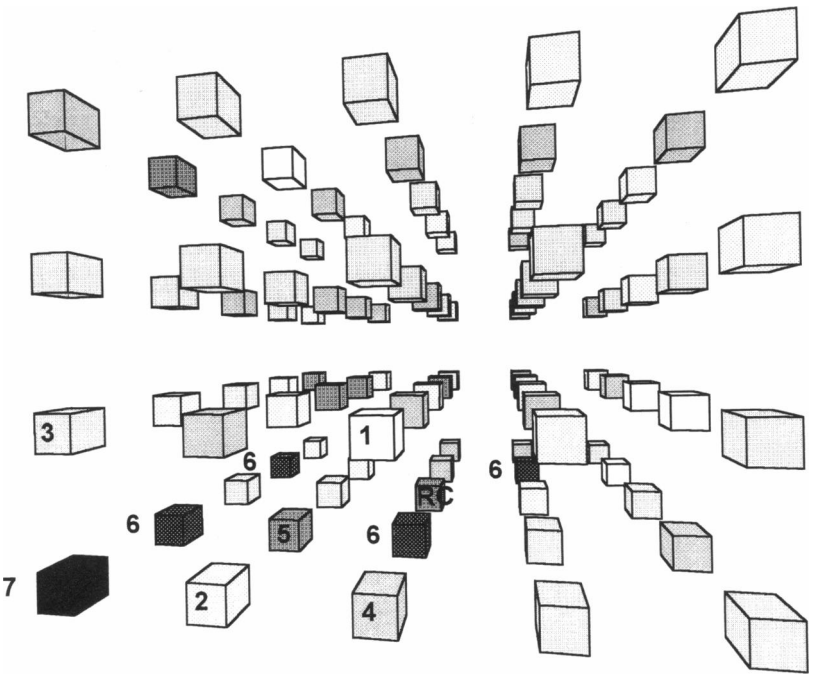

FIGURE 8 The optimal spatial distribution of the pigment spectral forms in the three-dimensional lattice model of PS I core particle obtained in the NNNR approximation. The optimal values for the continuous parameters are as follows: charge separation rate $k_{P700} = 1.8\ ps^{-1}$, lattice constant $a = 15.3$ Å, spacing between the P700 and the main pool pigments $a_{P700} = 7.4$ Å, spacing between the LWA pigments and the main pool pigments $a_{LWA} = 13.5$ Å. For the spectral content see the explanations in Fig. 4.

that the PS I system possesses some degree of flexibility in fulfilling the experimental restrictions with several different arrangements of pigments. This remains to be tested. Current experimental investigations may provide the required improved input data for the model. Later GA optimization runs then should also employ a substantially increased population size as compared to the one used here, to avoid the problems indicated in the Discussion. Given the present limited experimental data set, such costly optimization runs were not justified.

We thank Prof. K. Schaffner for support of this research and Mrs. I. Martin for valuable help with the computer system.

The research described in this publication was made possible in part by grant LE 6000 from the International Science Foundation to GT, and by a visiting fellowship to GT from the Deutsche Forschungsgemeinschaft (Sonderforschungsbereich 189, Heinrich-Heine-Universität Düsseldorf and the Max-Planck-Institut für Strahlenchemie, Mülheim a.d. Ruhr) and a visiting grant from the Max-Planck-Institut für Strahlenchemie.

REFERENCES

Beauregard, M., I. Martin, and A. R. Holzwarth. 1991. Kinetic modelling of exciton migration in photosynthetic systems. 1. Effects of pigment heterogeneity and antenna topography on exciton kinetics and charge separation yields. *Biochim. Biophys. Acta.* 1060:271–283.

Du, M., X. L. Xie, Y. W. Jia, L. Mets, and G. R. Fleming. 1993. Direct observation of ultrafast energy transfer in PSI core antenna. *Chem. Phys. Lett.* 201:535–542.

Fleming, G. R., and R. van Grondelle. 1994. The primary steps of photosynthesis. *Phys. Today* 47:48–55.

Freiberg, A., V. I. Godik, and K. Timpmann. 1987. Spectral dependence of the fluorescence lifetime of *Rhodospirillum rubrum*. Evidence for inhomogeneity of B880 absorption band. *In* Progress in Photosynthesis Research, Vol I. J. Biggins, editor. Marinus Nijhoff, Dordrecht, The Netherlands. 45–48.

Gobets, B., H. Van-Amerongen, R. Monshouwer, J. Kruip, M. Rögner, R. van Grondelle, and J. P. Dekker. 1994. Polarized site-selected fluorescence spectroscopy of isolated photosystem I particles. *Biochim. Biophys. Acta.* 1188:75–85.

Goldberg, D. E. 1989. Genetic Algorithms in Search, Optimization, and Machine Learning. Addison-Wesley, New York. 1–412.

Goldberg, D. E., and J. Richardson. 1987. Genetic algorithms with sharing for multimodal function optimization. *In* Genetic Algorithms and Their Applications. Proceedings of the Second International Conference on Genetic Algorithms. Morgan Kaufmann, San Mateo, CA. 41–49.

Holland, J. H. 1992. Adaptation in Natural and Artificial Systems. MIT Press, Cambridge, MA. 1–211.

Holzwarth, A. R. 1987. Picosecond fluorescence spectroscopy and energy transfer in photosynthetic antenna pigments. *In* The Light Reactions, Vol. 8. Topics in Photosynthesis. J. Barber, editor. Elsevier, Amsterdam. 95–157.

Holzwarth, A. R. 1991. Excited-state kinetics in chlorophyll systems and its relationship to the functional organization of the photosystems. *In* Chlorophylls. H. Scheer, editor. CRC Press, Boca Raton. 1125–1151.

Holzwarth, A. R. 1996. Data analysis of time-resolved measurements. *In* Biophysical Techniques. Advances in Photosynthesis Research. J. Amesz and A. Hoff, editors. Kluwer Academic, Dordrecht.

Holzwarth, A. R., and T. A. Roelofs. 1992. Recent advances in the understanding of chlorophyll excited state dynamics in thylakoid membranes and isolated reaction centre complexes. *J. Photochem. Photobiol. B.* 15:45–62.

Holzwarth, A. R., G. H. Schatz, H. Brock, and E. Bittersmann. 1993. Energy transfer and charge separation kinetics in photosystem I. 1. Picosecond transient absorption and fluorescence study of cyanobacterial photosystem I particles. *Biophys. J.* 64:1813–1826.

Jia, Y., J. M. Jean, M. M. Werst, C. Chan, and G. R. Fleming. 1992. Simulations of the temperature dependence of energy transfer in the PS I core antenna. *Biophys. J.* 63:259–273.

Karrasch, S., P. A. Bullough, and R. Ghosh. 1995. 8.5A projection map of the light-harvesting complex I from Rhodospirillum rubrum reveals a ring composed of 16 subunits. *EMBO J.* 14:631–638.

Krauss, N., W. Hinrichs, I. Witt, P. Fromme, W. Saenger, W. Pritzkow, Z. Dauter, C. Betzel, K. S. Wilson, and H. T. Witt. 1993. Three-dimensional structure of system I of photosynthesis at 6A resolution. *Nature.* 361:326–331.

Kühlbrandt, W., and D. N. Wang. 1991. Three-dimensional structure of plant light-harvesting complex determined by electron crystallography. *Nature.* 350:130–134.

Kühlbrandt, W., D. N. Wang, and Y. Fujiyoshi. 1994. Atomic model of plant light-harvesting complex by electron crystallography. *Nature.* 367: 614–621.

Laible, P. D., W. Zipfel, and T. G. Owens. 1994. Excited state dynamics in chlorophyll-based antennae: the role of transfer equilibrium. *Biophys. J.* 66:844–860.

Lin, S., H.-C. Chiou, F. A. M. Kleinherenbrink, and R. E. Blankenship. 1994. Time-resolved spectroscopy of energy and electron transfer processes in the photosynthetic bacterium *Heliobacillus mobilis. Biophys. J.* 66:437–445.

McDermott, G., S. M. Prince, A. A. Freer, M. Papiz, A. M. Hawthornthwaite-Lawless, R. J. Cogdell, and N. W. Isaacs. 1995. Crystal structure of an integral membrane light-harvesting complex from photosynthetic bacteria. *Nature.* 374:517–521.

Oliver, I. M., D. J. Smith, and J. R. C. Holland. 1987. A study of permutation crossover operators on the traveling salesman problem. *In* Genetic Algorithms and Their Applications. Proceedings of the Second International Conference on Genetic Algorithms. Morgan Kaufmann, San Mateo, CA. 224–230.

Parson, W. W. 1991. Reaction centers. *In* Chlorophylls. H. Scheer, editor. CRC Press, Boca Raton. 1153–1180.

Pearlstein, R. M. 1982. Exciton migration and trapping in photosynthesis. *Photochem. Photobiol.* 35:835–844.

Pullerits, T., K. J. Visscher, S. Hess, V. Sundström, A. Freiberg, K. Timpmann, and R. van Grondelle. 1994. Energy transfer in the inhomogeneously broadened core antenna of purple bacteria: a simultaneous fit of low-intensity picosecond absorption and fluorescence kinetics. *Biophys. J.* 66:236–248.

Shiozawa, J. A., R. S. Alberte, and J. P. Thornber. 1974. The P700-chlorophyll a-protein. Isolation and some characteristics of the complex in higher plants. *Arch. Biochem. Biophys.* 165:388–397.

Somsen, O. J. G. 1995. Excitonic interaction in photosynthesis. Migration and spectroscopy. Ph.D. Thesis. Free University of Amsterdam.

Somsen, O. J. G., F. van Mourik, R. van Grondelle, and L. Valkunas. 1994. Energy migration and trapping in a spectrally and spatially inhomogeneous light-harvesting antenna. *Biophys. J.* 66:1580–1596.

Sundström, V., and R. van Grondelle. 1991. Dynamics of excitation energy transfer in photosynthetic bacteria. *In* Chlorophylls. H. Scheer, editor. CRC Press, Boca Raton. 1097–1124.

Trinkunas, G., and A. R. Holzwarth. 1994a. Kinetic modeling of exciton migration in photosynthetic systems. 2. Simulations of excitation dynamics in two-dimensional photosystem I core antenna/reaction center complexes. *Biophys. J.* 66:415–429.

Trinkunas, G., and A. R. Holzwarth. 1994b. Modelling of energy transfer in photosystem I using genetic algorithm. *Liet. Fiz. Zurn.* 34:287–292.

Trissl, H.-W. 1993. Long-wavelength absorbing antenna pigments and heterogeneous absorption bands concentrate excitons and increase absorption cross section. *Photosynth. Res.* 35:247–263.

Trissl, H.-W., B. Hecks, and K. Wulf. 1993. Invariable trapping times in photosystem I upon excitation of minor long-wavelength absorbing pigments. *Photochem. Photobiol.* 57:108–112. (Abstr.)

Valkunas, L., S. Kudzmauskas, and V. Liuolia. 1986. Noncoherent migration of excitation in impure molecular structures. *Sov. Phys. Collect. (Liet. Fiz. Rink).* 26:1–11.

Valkunas, L., V. Liuolia, J. P. Dekker, and R. van Grondelle. 1995. Description of energy migration on photosystem I by a model with two distance scaling parameters. *Photosynth. Res.* 43:149–154.

van der Laan, H., T. Schmidt, R. W. Visschers, K. J. Visscher, R. van Grondelle, and S. Völker. 1990. Energy transfer in the B800–850 antenna complex of purple bacteria *Rhodobacter sphaeroides*: a study by spectral hole-burning. *Chem. Phys. Lett.* 170:231–238.

van der Lee, J., D. Bald, S. L. S. Kwa, R. van Grondelle, M. Rögner, and J. P. Dekker. 1993. Steady-state polarized light spectroscopy of isolated photosystem-I complexes. *Photosynth. Res.* 35:311–321.

van Grondelle, R., J. P. Dekker, T. Gillbro, and V. Sundström. 1994. Energy transfer and trapping in photosynthesis. *Biochim. Biophys. Acta.* 1187:1–65.

Weiss, G. H. 1967. First passage time problems in chemical physics. *Adv. Chem. Phys.* 13:1–18.